



Research Article

## Entropy generation of $Al_2O_3$ /water nanofluid in corrugated channels

Leila SAOUDI<sup>1,\*</sup>, Nordine ZERAIBI<sup>1</sup>

<sup>1</sup>Laboratory of Engineering Physics Hydrocarbons, University M'hamed Bougara Boumerdes, 35000, Algeria

### ARTICLE INFO

#### Article history

Received: 06 November 2022

Revised: 07 April 2023

Accepted: 11 April 2023

#### Keywords:

Entropy Generation; Laminar Flow; Nanofluid; Sinusoidal and Square Channel

### ABSTRACT

The flow of nanofluids in a corrugated channel has been shown to have a significant impact on heat transfer performance, and has therefore become an important area of research. The objective of this paper is to understand the thermal behavior of  $Al_2O_3$ /water nanofluid in a sinusoidal and square channel and to identify ways to optimize heat transfer performance in such configurations. For this purpose, a numerical simulation was conducted using ANSYS-Fluent software 16.0 on entropy generation and thermo-hydraulic performance of a wavy channel with the two corrugation profiles (sinusoidal and square). The analyses were carried out under laminar forced convection flow conditions with constant heat flux boundary conditions on the walls. The influence of various parameters, such as particle concentration (0–5%), particle diameter (10nm, 40nm and 60nm), and Reynolds number ( $200 < Re < 800$ ) on the heat transfer, thermal, and frictional entropy generation, and Bejan number was analyzed. Moreover, the distribution of streamlines and static temperature contours has been presented and discussed, and a correlation equation for the average Nusselt number based on the numerical results is presented. One of the most significant results obtained is that the inclusion of nanoparticles (5% volume fraction) in the base fluid yielded remarkable results, including up to 41.92% and 7.03% increase in average Nusselt number for sinusoidal and square channels, respectively. The sinusoidal channel exhibited the highest thermo-hydraulic performance at  $Re = 800$  and  $\phi = 5\%$ , approximately  $THP = 1.6$ .

In addition, the increase of nanoparticle concentration from 0% to 5% at  $Re = 800$  and  $d_{np} = 10nm$ , diminishes the total entropy generation by 28.39 % and 22.12 % for sinusoidal and square channels, respectively, but when the nanoparticle diameter decreases from 60nm to 10nm at  $\phi = 5\%$  and  $Re = 800$ , the total entropy generation in the sinusoidal channel decreases by 34.85%, whereas in the square channel, it decreases by 20.05%. Therefore, rather than using a square channel, it is preferable and beneficial to use small values of nanoparticle diameter and large values for each of  $\phi$  and  $Re$  in the sinusoidal wavy channel. Overall, the study of nanofluid flow in a wavy channel can provide valuable insights into the behavior of nanofluids and their potential applications in a variety of fields, including manufacturing, energy production, mining, agriculture, and environmental engineering.

**Cite this article as:** Saoudi L, Zeraibi N. Entropy generation of  $Al_2O_3$ /water nanofluid in corrugated channels. J Ther Eng 2023;9(4):885–900.

#### \*Corresponding author.

\*E-mail address: [l.saoudi@univ-boumerdes.dz](mailto:l.saoudi@univ-boumerdes.dz)

This paper was recommended for publication in revised form by Assigned Editor Ahmet Selim Dalkilic



## INTRODUCTION

The enhancement of heat transfer performance in a straight channel is crucial for energy conservation, and several approaches have been suggested by authors to achieve this. These include the implementation of diverse surface geometries [1] and the addition of solid nanoparticles with high thermal conductivities [2, 3].

Nanofluids, which are suspensions of nanoparticles in conventional fluids, are attracting considerable attention due to their unique characteristics, such as enhanced thermal conductivity, improved heat transfer performance [4], and increased thermal stability. As a result, they are utilized in various industrial and energy applications, such as thermal engineering, the design of heat exchangers [5], radiators and other heat transfer equipment for various applications, including electronic cooling, power generation and solar energy collection.

Our research specifically investigates the use of  $\text{Al}_2\text{O}_3$  nanoparticles, which have been used in other studies involving the dispersion of nanoparticles in base fluids. Among all the studies using  $\text{Al}_2\text{O}_3$  nanoparticles, we can cite the investigation of Ekiciler, R. [6] on the numerical study of  $\text{Al}_2\text{O}_3$ /water forced convection nanofluid flow in a duct with a backward-facing step. The nanoparticle volume fraction was varied between 1% and 5%, and the Reynolds number was increased from 100 to 500. The study examined Nusselt number, velocity profiles, and friction factor in detail, and found that the Nusselt number increases with increasing nanoparticle volume fraction and Reynolds number. As we can also mention the study of Sattar Aljabair et al. [7], the authors present a numerical study of natural convection heat transfer in corrugated annuli filled with a nanofluid  $\text{Al}_2\text{O}_3$ /water. The results showed that an increase in nanoparticles volume fraction and Rayleigh number led to a significant increase in heat transfer rates. The study also deduced correlations for the mean Nusselt number. The research conducted by Kaya, H. et al. [8] investigated the impact of nanoparticle concentration on heat transfer efficiency using suspended  $\text{Al}_2\text{O}_3$  nanoparticles in pure water. The study analyzed various parameters that affect heat transfer efficiency, including nanoparticle diameter and Reynolds number. Furthermore, the research found that a specific configuration (U-tube solar collector) was more efficient for heat transfer than alternative configurations. Another study worth mentioning is the study of Ekiciler, R. et al. [9], who discusses a numerical study of forced convective heat transfer in a three-dimensional equilateral triangular duct using  $\text{Al}_2\text{O}_3$ /water nanofluid with different shapes of nanoparticles and varying nanoparticle volume fractions. The study aims to determine how different nanoparticle shapes and volume fractions affect heat transfer and flow features, analyzing parameters such as convective heat transfer coefficient, Nusselt number, Darcy friction factor, pumping power, and performance evaluation criterion

(PEC) in the duct. The results show that the platelet nanoparticle shape produces the greatest heat transfer enhancement, and heat transfer in the duct increases with increasing nanoparticle volume fraction.

Extensive research has been conducted on forced convective flow using traditional fluids in various configurations with wavy walls [10]. This is because wavy surfaces enhance the mixing process between hot and mainstream fluids due to growing separation zones near the wavy walls, ultimately improving heat transfer performance. Wavy channels are commonly used in fluid mechanics experiments, as well as in the production of textiles, paper, and oil and gas pipelines to increase flow efficiency and reduce vibrations. Additionally, wavy channels are beneficial in agriculture for controlling water flow to crops, leading to efficient irrigation. Wang et al. [11] examined the heat transfer of flow through a sinusoidally curved converging-diverging channel and found that the flow in such channels improved heat transfer, albeit with an increase in pressure drop compared to straight channels.

In the field of nanofluids, recent research has concentrated on examining the thermal properties of nanofluid flow in a channel with wavy features. The flow of nanofluids in such a channel has been shown to have a significant influence on heat transfer performance, making it a crucial area of investigation with several potential contributions to various fields, including enhanced mixing, improved fluid dynamics, improved fluid-structure interaction, and enhanced heat transfer. To optimize heat transfer in engineering applications, several researchers have suggested the use of nanofluids in channels featuring corrugated surfaces. The aim of Sattar Aljabair et al. [12] research is to expand and investigate the issue of mixed convection of nanofluids in a cavity with an arc shape. This cavity is propelled by a sinusoidal lid, and its lower wall has a sinusoidal temperature variation. The findings reveal that an increase in Reynolds number, Rayleigh number, and the volumetric fraction of Cu nanoparticles results in higher local and average heat transfer rates. Additionally, the study presents correlation equations for the average Nusselt number. The study of Gürsoy, E. et al. [13], focuses on the use of nanofluids to enhance heat transfer in sudden expansion geometries, which are often employed in heat exchangers. Numerical analyses were performed on different expansion ratios, Reynolds numbers ranging from 100 to 2000, a constant and uniform heat flux of  $600 \text{ W/m}^2$ , and volume concentrations of nanofluids ranging from 1.0 to 2.0 vol.%. The results indicate that using a dimpled tube is more effective in improving heat transfer, and optimal performance is achieved at a volume concentration of 2.0 vol.%. Compared to water, the highest increase in the Nusselt number was obtained at  $\text{Re}=2000$  and  $\phi=2.0$  vol.%. Furthermore, the convective heat transfer rate is higher on the bottom wall of the dimpled tube than on the top wall. The study by Ahmed S. Habeeb et al. [14] explores the use of a hybrid

nano-fluid made of 50%  $\text{Fe}_3\text{O}_4$  and 50%  $\text{MgO}/\text{H}_2\text{O}$ , with varying volume concentrations of 0.5%, 1%, and 2%, to enhance heat transfer in plain and wavy tubes under turbulent flow and constant heat flux conditions. The study involves experimental investigation and numerical simulation to analyze the flow field, migration of nanoparticles volume fraction effect, and heat transfer. The results show that increasing Reynolds numbers and volume fractions of the hybrid nano-fluid lead to lower friction factor and greater enhancement in heat transfer and performance evaluation criteria than the conventional base fluid. The highest Nusselt number is observed at 2% of ( $\text{Fe}_3\text{O}_4$ ). In study of Noor F. et al. [15], the authors present an experimental and numerical study to investigate the heat transfer enhancement in a horizontal circular tube using a hybrid nanofluid ( $\text{CuO}$ ,  $\text{Al}_2\text{O}_3$ /distilled water) and fitted with twisted tape. The study finds that the hybrid nano-fluid with twisted tape shows maximum enhancement in the maximum thermal performance factor of 2.18 for  $\phi=1.8\%$ , while for a tube (water with twisted) under the same conditions, it was 2.04. The concentration of 1.8% hybrid nanofluid shows a high Nusselt number and an enhancement in heat transfer of about 6.70% compared to water.

The study by Albojamal et al. [16] focused on the flow of nanofluids inside a horizontal tube and a corrugated channel under a constant wall temperature boundary condition. They investigated single-phase and two-phase models for  $\text{Al}_2\text{O}_3$  and  $\text{CuO}$ -water nanofluids, considering the effect of constant and temperature-dependent thermophysical properties. The authors concluded that the homogeneous single-phase model can be used in nano-fluid flow studies to obtain results with acceptable accuracy, without the need to use the more computationally expensive two-phase models. H. Heidary et al. [17] performed a numerical investigation of laminar forced convective flows of  $\text{Cu}$ /water nanofluid under a constant wall temperature boundary condition through a wavy channel. The influences of various parameters, such as nanofluid volume fraction ( $0 \leq \phi \leq 20\%$ ), wave amplitude ( $0 \leq \alpha \leq 0.3$ ), and Reynolds number (5-1500) were analyzed and discussed in detail. It is concluded that the addition of nanoparticles and the usage of wavy horizontal walls can enhance heat transfer by 50%.

In recent years, nanofluids have received much attention as a promising solution for improving heat transfer in various industrial applications (Biomedical engineering, Automotive, Energy and power generation). As a result, there has been a surge of research on thermal and frictional entropy generation of nanofluids flow in various channel configurations, including corrugated channels, with the aim of acquiring more information about the quality of energy available in any system.

The most important work that can be cited is the study by Mahian et al. [18] who presented a review of entropy generation of the flow of nanofluids in different regimes, summarizing the work found in the literature from the

year 2010 to 2013. The essential result of this work showed that the use of nanoparticles in base fluids improves heat transfer and reduces entropy generation. In addition, we can mention the Taskesen et al. [19] study who presented the numerical results of forced convection of laminar  $\text{Fe}_3\text{O}_4$ /water flow in cylindrical, square, rectangular, and triangular channel cross-sections. The effects of some parameters (Reynolds number, nanoparticle volume fractions, channel geometries) on the mean Nusselt number, Darcy friction factor, and entropy generation were studied in detail.

In addition, we can mention the work of Pazarlıoğlu, H. K. et al. [20], their paper presents a computational study of the thermo-hydraulic performance and entropy generation of a sudden expansion tube with elliptical dimpled fins (DFs) using cobalt ferrite/ $\text{H}_2\text{O}$  nanofluid. The study investigates the effect of the elliptical DF and its arrays on thermodynamic laws and performance evaluation criteria at different Reynolds numbers and volumetric concentrations. The results show that the use of elliptical DFs in a sudden expansion tube enhances convective heat transfer rate and decreases total entropy generation. The study offers extensive numerical data and results that can be used for further analysis and research in various industries, such as Thermal Power Generation, Chemical Engineering, Automotive Engineering, and Manufacturing. The results obtained can aid in optimizing the manufacturing processes of heat exchangers and other related components, leading to cost reduction and improved product quality. As we can add the study of Pazarlıoğlu, H. K. et al. [21] which has as an application area the solar thermal energy systems. Specifically, the study focuses on improving the performance of parabolic trough collectors, which are commonly used in concentrating solar power plants to generate electricity from solar energy. The results of this study can be used to optimize the design and performance of parabolic trough collectors to make them more efficient and cost-effective for renewable energy production. The influence of Reynolds number and different wall undulation profiles (sinusoidal, trapezoidal, and triangular) on the entropy generation of water flow in a corrugated channel has been studied by M. Akbarzadeh et al. [22]. The results of their analysis were examined and compared with those of a straight channel. According to the results of this work, a sinusoidal wall is suitable for use in a channel. S. Rashidi et al. [23] studied the influence of Reynolds number (5000-50,000), wavelength of the corrugated wall (1, 2, and 3), and wave amplitude (0.1, 0.2, and 0.3) on heat transfer, pressure drop, and thermal and frictional irreversibility for water flow.

In addition to studies using the minimization approach of entropy generation in the case of base fluid flow in a wavy channel, few experimental and numerical studies in the case of corrugated channels with nanofluids have been undertaken. We can cite the study that was carried out by Ansys-Fluent on a  $\text{Cu}$ -water nanofluid through

a corrugated channel on a heat exchanger plate by J.A. Esfahani et al. [24], using second law analysis. The effects of different parameters such as dimensionless amplitude (0.1-0.3), nanoparticle concentration (0.01-0.05), wave number (4-8) and Reynolds number ( $300 < Re < 900$ ) on the entropy generation rates (viscous, thermal, total) and the Bejan number are studied. Our results are consistent with their results regarding the effect of Reynolds number and nanoparticle volume concentration on viscous and thermal entropy generation because, according to them, thermal entropy generation decreases and viscous entropy generation increases with the volume fraction of nanoparticles, and the total entropy generation decreases with increasing Reynolds number. In addition to these results, we studied the effect of nanoparticle size, which to my knowledge has not been studied yet in this type of research. The results of our study are in agreement with the results found by H. Hudhaifa and S. B. Sahin [25] in the case of SWCNT/water nanofluid flow in a sinusoidal corrugated channel, where the authors showed that the use of a high volume fraction improves heat transfer and decreases thermal irreversibility in the considered channel. B. Boudraa and R. Bessaih [26] presented numerical results of laminar flow with forced convection of water-TiO<sub>2</sub> nanofluid. The study was conducted using a two-phase mixing model for a corrugated channel under constant heat flux. The study examined the influence of different parameters ( $a$ ,  $\phi$ , and  $Re$ ) on flow behavior, heat transfer, and frictional and thermal entropy generation. According to their results, the heat transfer rate improves when  $a$ ,  $Re$ , and  $\phi$  increase. Moreover, the thermal entropy generation decreases while the frictional entropy generation increases as  $\phi$  and  $Re$  increase.

Due to the lack of knowledge in the area of entropy generation in wavy channels, the originality of our work consists of analyzing the effect of nanoparticle diameter on entropy generation. To the best of our knowledge, the influence of nanoparticle size on entropy generation in a corrugated channel has not been extensively studied. Additionally, we compare the results of entropy generation between a corrugated square and a sinusoidal channel. This study will help us choose the most suitable channel in terms of heat transfer improvement and entropy generation minimization. Moreover, we propose a correlation of Nusselt number as a function of nanoparticle concentration and Reynolds number for the nanoparticle size of 10 nm at the sinusoidal and square channel, respectively.

Below is a possible workflow for conducting a numerical investigation using the Fluent software to examine the entropy generation of a nanofluid consisting of Al<sub>2</sub>O<sub>3</sub> and water in channels with corrugated surfaces:

1. Define the problem:
  - Define the geometry of the corrugated channel, including its dimensions and shape.
  - Specify the fluid properties of the Al<sub>2</sub>O<sub>3</sub> / water nanofluid, such as density, viscosity, and thermal conductivity.

- Determine the boundary conditions for the flow and heat transfer.
2. Mesh generation:
    - Create a mesh of the corrugated channel geometry.
    - Ensure that the mesh is sufficiently fine to accurately capture the flow and heat transfer behavior.
  3. Solver setup:
    - Select the appropriate solver settings for the simulation, such as the type of fluid flow and convergence criteria.
  4. Simulation:
    - Run the simulation using the chosen solver settings and models.
    - Monitor the convergence of the solution and adjust the solver settings if necessary.
    - Evaluate the results of the simulation.
  5. Post-processing:
    - Use Fluent's post-processing tools to visualize and analyze the simulation results.
    - Calculate the entropy generation and other relevant quantities, such as the average Nusselt number.
    - Plot and compare the results for different cases or scenarios, such as varying the nanofluid concentration, nanoparticle diameter or channel geometry.
  6. Interpretation and conclusion:
    - Interpret the simulation results and draw conclusions about the behavior of the Al<sub>2</sub>O<sub>3</sub>/water nanofluid in corrugated channels.
    - Consider future directions for research or development based on the findings.

## MATHEMATICAL FORMULATION

### Description of the Problem

As it can be seen in Figure 1, geometric parameters of the calculation model are taken as given by S. Rashidi et al. [23], the length of the channels is  $L = 20H$ , the height between the lower and upper walls is “2H”, the ripple amplitude is  $a = 0.2H$  and the wavelength  $L_w = 2H$ . Two sections of smooth adiabatic wall of length “3H” and “5H” are imposed respectively at the beginning and at the end of the corrugated wall, which is under a constant heat flux and comprises six corrugated units with a length of “12H”.

Geometric shape of upper sinusoidal and square corrugated walls are defined respectively by Equations 1 and 2.

$$S(x) = H + a \sin\left(\frac{\pi(x-3H)}{H}\right), \quad 3H < x < 15H \quad (1)$$

$$S(x) = \begin{cases} H+a & ; 3H+nL_w \leq x \leq 3H+(n+1)L_w \quad ; n=0,2,4,6,8,10 \\ H-a & ; 3H+nL_w < x < 3H+(n+1)L_w \quad ; n=1,3,5,7,9 \end{cases} \quad (2)$$

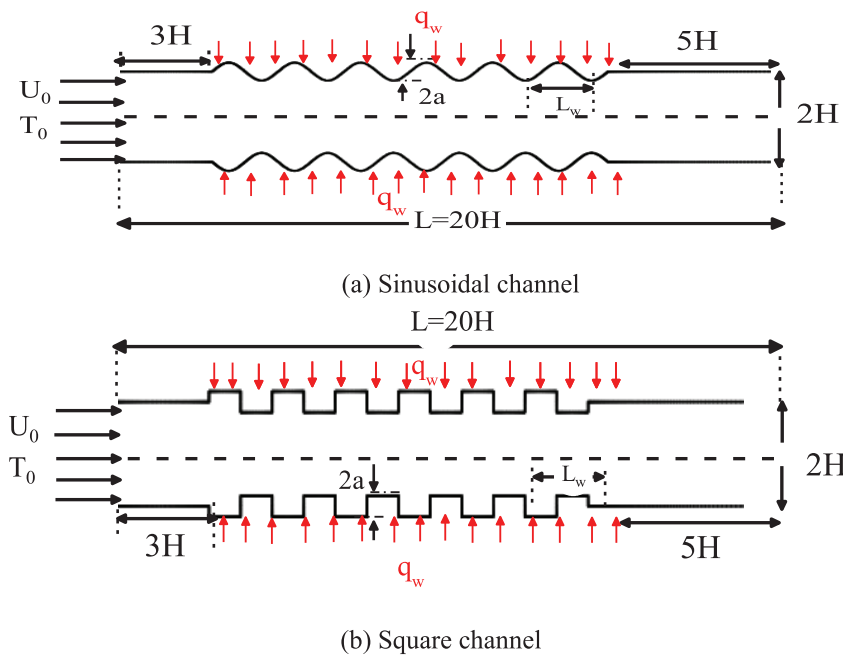


Figure 1. Schematic configuration of the two wavy channels.

**Boundary conditions**

The boundary conditions summarized in table1 are applied to solve the equations governing the flow studied in this work. Uniform velocity which depends on the Reynolds number and a constant temperature are defined at the wavy channel inlet, and The Neumann boundary conditions are defined at the exit of the wavy channel (all gradients are

equal to zero). The wavy wall is exposed to heat flow, and all walls are adiabatic.

The properties of water used as base fluid in this work depend on temperature, estimated from polynomial models of Ebrahimnia et al. [27] ( valid properties in the range  $(294 \leq T(K) \leq 324)$ ). Note that the channels were filled with  $Al_2O_3$ /water nanofluid , where thermo-physical properties of the used nanoparticle and water are found in Table 2.

Table 1. Boundary conditions

Boundary conditions	U (m/s)	V(m/s)	T(K)	$q_w (W/m^2)$
Inlet	$U_{in}$	0	298	-
Wavy walls	0	0	-	5000
Smooth walls	0	0	-	0
Outlet	$\frac{\partial u}{\partial x} = 0$	$\frac{\partial v}{\partial x} = 0$	$\frac{\partial T}{\partial x} = 0$	-

Table 2. Thermo-physical properties of Water [27] and considered nanoparticles metal oxide ( $Al_2O_3$ ) [28].

Properties	Water	$Al_2O_3$
$\rho$ (kg/m <sup>3</sup> )	$\rho_{bf} = -3 \times 10^{-3} T^2 + 1,505 T + 816,781$	3970
CP (J/kg k)	$C_{bf} = -4,63 \times 10^{-6} T^3 + 5,52 \times 10^{-2} T^2 - 20,86 T + 6719,637$	765
k (w/mk)	$k_{bf} = -7,843 \times 10^{-6} T^2 + 6,2 \times 10^{-3} T - 0,54$	40
$\mu$ (mPa.s)	$\mu_{bf} = 2.414 \times 10^{-5} \times 10^{(247,8/(T-140))}$	-

### Governing Equations

The resulting mixtures of water and nanoparticle, assumed to be in thermal equilibrium, are treated as a single-phase fluid [29]. Assumptions considered in this study with the single-phase approach include:

- The fluid is incompressible and Newtonian.
- The flow is laminar and steady-state.
- The nanofluid is homogeneous and isotropic.
- The nanoparticles are supposed to be spherical form.

These assumptions simplifies the modeling of nanofluid flow and heat transfer.

The equations governing the nanofluid flow are:

Continuity equation:

$$\frac{\partial u}{\partial x} + \frac{\partial v}{\partial y} = 0 \quad (3)$$

Momentum equation in x direction is given by:

$$\rho_{nf} \left( u \frac{\partial u}{\partial x} + v \frac{\partial u}{\partial y} \right) = -\frac{\partial p}{\partial x} + \mu_{nf} \left( \frac{\partial^2 u}{\partial x^2} + \frac{\partial^2 u}{\partial y^2} \right) \quad (4)$$

Momentum equation in y direction is given by:

$$\rho_{nf} \left( u \frac{\partial v}{\partial x} + v \frac{\partial v}{\partial y} \right) = -\frac{\partial p}{\partial y} + \mu_{nf} \left( \frac{\partial^2 v}{\partial x^2} + \frac{\partial^2 v}{\partial y^2} \right) \quad (5)$$

Energy equation:

$$\rho_{nf} C_{p,nf} \left( u \frac{\partial T}{\partial x} + v \frac{\partial T}{\partial y} \right) = K_{nf} \left( \frac{\partial^2 T}{\partial x^2} + \frac{\partial^2 T}{\partial y^2} \right) \quad (6)$$

### Nanofluid thermo-physical properties

Al<sub>2</sub>O<sub>3</sub> nanoparticles are commonly used in forced convection flows due to their unique physical and chemical properties (high thermal conductivity, high specific surface area, chemical stability) in addition to their availability and low cost which make them well suited for this application.

The physical and thermal properties of nanofluids can be defined as follows:

Pak and Cho's relation [30] was used for the calculation of the density of nanofluids:

$$\rho_{nf} = \rho_p \phi + \rho_{bf} (1 - \phi) \quad (7)$$

Using the relation of Xuan and Roetzel [31], heat capacity of the two studied nanofluids was estimated by Eq. (8) as:

$$(C_p \rho)_{nf} = \phi (C_p \rho)_p + (1 - \phi) (C_p \rho)_{bf} \quad (8)$$

The model proposed by Corcione [32] was used to evaluate the thermal conductivity of nanofluids as follows:

$$k_{nf} = k_{bf} \left( 1 + 4,4 \text{Re}_p^{0,4} \text{Pr}_f^{0,66} \left( \frac{T}{T_{fr}} \right)^{10} \left( \frac{k_p}{k_{bf}} \right)^{0,03} \phi^{0,66} \right) \quad (9)$$

With the Reynolds number "Rep" of nanoparticles is defined as:

$$\text{Re}_p = \frac{2\rho_f K_b T}{\pi \mu_f^2 d_{np}} \quad (10)$$

The following expression proposed by Rudyak [33] (see Eq. (10)) was used to determine dynamic viscosity of nanofluids.

$$\mu_{nf} = \mu_{bf} \left( 1 + (2.5 + 13.43 e^{-0.013 \frac{d}{d_{bf}}}) \phi + (7.35 + 38.33 e^{-0.013 \frac{d}{d_{bf}}}) \phi^2 \right) \quad (11)$$

### First and Second Law of Thermodynamics Analysis

Equation (12) expresses the representative dimensionless heat transfer number (Nusselt number) as follows:

$$Nu(x) = \frac{h(x) \cdot D}{k_{nf}} = \frac{q_w \cdot D}{(T_w(x) - T_b(x)) k_{nf}} \quad (12)$$

$$Nu_{ave} = \frac{1}{L} \int_0^L Nu(x) dx \quad (13)$$

The ratio of heat transfer performance to friction factor, defined by Eq. (14), is used to achieve thermo-hydraulic performance.

$$THP = \frac{(\overline{Nu_{nf}} / \overline{Nu_{bf}})}{(f_{nf} / f_{bf})^{1/3}} \quad (14)$$

According to equations derived from Bejan [34, 35], entropy generation in a system includes thermal and frictional entropy; the analysis of both types of entropies is very important in engineering (energy conversion and storage devices and heat exchangers [36]). Thermal and frictional entropy generations are defined below:

$S_t'''$  is the local volumetric entropy generation rate due to heat transfer that is calculated by:

$$S_t''' = \frac{K_{nf}}{T^2} \left[ \left( \frac{\partial T}{\partial x} \right)^2 + \left( \frac{\partial T}{\partial y} \right)^2 \right] \quad (15)$$

$S_f'''$  is the local volumetric entropy generation rate caused by fluid flow and friction, that is calculated by:

$$S_f''' = \frac{\mu_{nf}}{T} \left\{ 2 \left[ \left( \frac{\partial u}{\partial x} \right)^2 + \left( \frac{\partial v}{\partial y} \right)^2 \right] + \left[ \left( \frac{\partial u}{\partial y} \right) + \left( \frac{\partial v}{\partial x} \right) \right]^2 \right\} \quad (16)$$

Volumetric total entropy generation is defined as the following relation:

$$S_{tot}''' = S_t''' + S_f''' \quad (17)$$

By integration of  $S_{tot}'''$  over the totality of the domain ( $\Omega$  is the solution domain), total entropy generation is calculated with the aim of analysing and understanding the flow characteristics of the fluid by addition of nanoparticles [37].

$$S_{tot} = \int_{\Omega} S_{tot}''' d\Omega = \int_{\Omega} (S_t''' + S_f''') d\Omega = S_t + S_f \quad (18)$$

The Bejan number is defined as the ratio of the thermal entropy generation to total entropy generation. Bejan number can be defined by:

$$Be = \frac{S_t}{S_{tot}} = \frac{S_t}{S_t + S_f} \quad (19)$$

### NUMERICAL METHOD

The equations governing laminar forced convection flow of nanofluids in corrugated channels have been solved numerically by finite volume method [38]. Second order upwind scheme is used to obtain precise results for momentum and energy equations. Moreover the pressure velocity coupling was resolved by SIMPLE algorithm.

The convergence criterion is fixed at 10-7 for (U,V,P) and 10-12 for T. Computational Fluid Dynamics (CFD) based FLUENT 16.0 [39] program was used for numerical solutions but, I introduced my personal program for the calculation of frictional, thermal, and total entropy generation, as I introduced personal User-Defined Functions (UDFs) that calculate the thermophysical properties that depend on the temperature of the water.

### Grid Independence Test and Validation

Validation of laminar flow regime in a nanofluid through a wavy channel is crucial in numerical modeling. Tests include grid independence, numerical convergence, and comparison to experimental data to ensure accurate predictions. Once validated, the model can investigate flow and heat transfer characteristics for various applications. A non-uniform rectangular grid with a very fine spacing near the walls, as shown in Figure 2, were used in the mesh structure of the numerical model. Various tests for both channels were applied for grid independence at cell numbers of 19200, 32000, 38400, 48000. After 38400 element numbers, the difference between Nusselt average was determined to be less than 2%. Therefore, the element number of 38400 was adopted for the numerical model. The variation of the cell numbers and Nusselt numbers were given in Table 3.

Still in the context of the validation of the present study, the accuracy of the grid was verified by comparing the average Nusselt number obtained with the total number of meshes corresponding to 38400 by this study with the numerical and experimental results presented respectively by Akbarzadeh et al. [22] and Ahmed et al. [40], Figure 3 shows that the three results agree well. Moreover, we observe in Figure 4, that the local Nusselt number has the highest value on the first wave of the channel and then it decreases along the channel until the fourth wave, after

**Table 3.** The Results of Grid Independence Test. (Re=800, for base fluid)

Test	Mesh size	Nuave Sinusoidal channel	Nuave Square channel
1	19200	26.421	21.012
2	32000	25.761	19.578
3	38400	21.952	19.225
4	48000	21.553	19.219

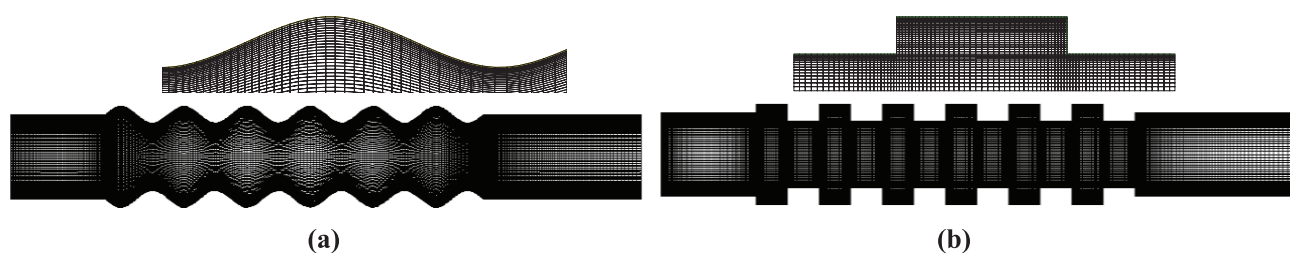


**Figure 2.** Schematic view of the adopted grid for: (a) sinusoidal channel, (b) square channel.

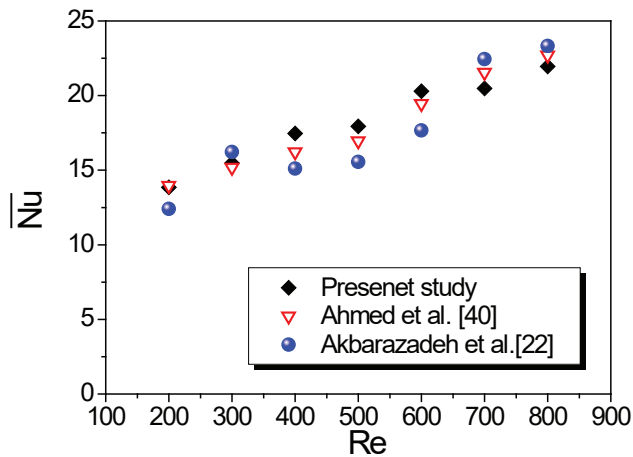


**Figure 3.** Comparison of the average Nusselt number versus Reynolds numbers at  $\phi=0$  and  $\lambda=0.2$  with the previous data [40,22].

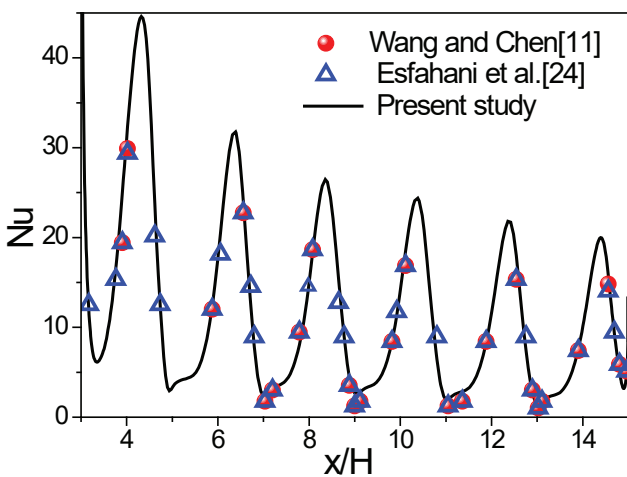


**Figure 4.** Comparison of the local Nusselt number at  $\phi=0$ ,  $Re=500$  and  $\lambda=0.2$  for a sinusoidal channel with the results of Wang and Chen [11] and Esfahani et al. [24].

that, the variation of the Nusselt number with the increase of the axial distance is negligible, due to the formation of the thermal boundary layer. A reasonable agreement can be seen by comparing this result with the numerical results published by Wang and Chen [11] and Esfahani et al. [24].

### RESULTS AND DISCUSSION

In the first part of the numerical results, effect of the geometry of the pipe (sinusoidal and square wavy channels) on the evolution of the current function, the temperature field and the local and average Nusselt number is evaluated and discussed.

#### Analysis of Flow and Temperature Fields

This section presents the results of the analysis of Streamlines contours and isothermal contours in the channel to explain the flow and heat transfer mechanism.

Figures 5 disclose the streamlines for sinusoidal and square ducts of  $Al_2O_3$ -water nanofluid at  $Re=200$  and  $Re=800$  at a constant particle volume fraction ( $\phi=0.05$ ). The presence of reverse flows in the divergent section of the corrugated conduit leads to recirculation zones, whose size depends on the shape of the channel. So channel with sinusoidal corrugation profile has the largest recirculation region relative to the square one. As we can see that the strength and length of the recirculation zones formed between the waves (divergent regions) increase with  $Re$ . It should be noted that near the walls of the corrugated channels, at the level of the recirculation zones which improve the mixing of the cold fluid with the hot one, the flow disturbances are much stronger. Similar observation for the case of pure water can be found in the study of Akbarzadeh et al. [22].

Figure 6 presents the isothermal contours of the sinusoidal and square channels for  $Re=200$  and  $Re=800$ . The figure illustrates that the temperature gradient in the vicinity of the heated wall increases as the Reynolds number increases. This is due to the improved quality of the flow

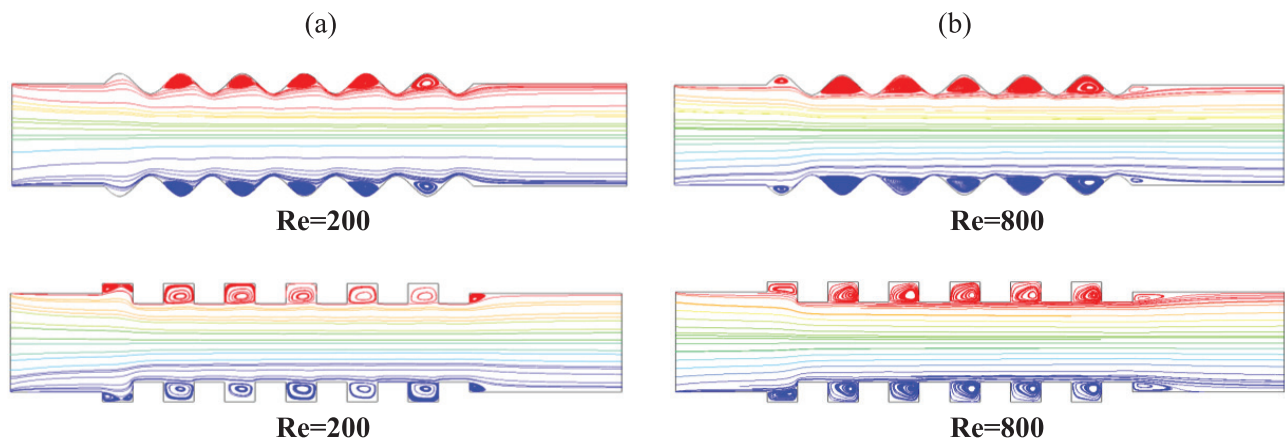


**Figure 5.** Streamlines contours at (a)  $Re=200$ , (b)  $Re=800$  for  $f=5\%$ .



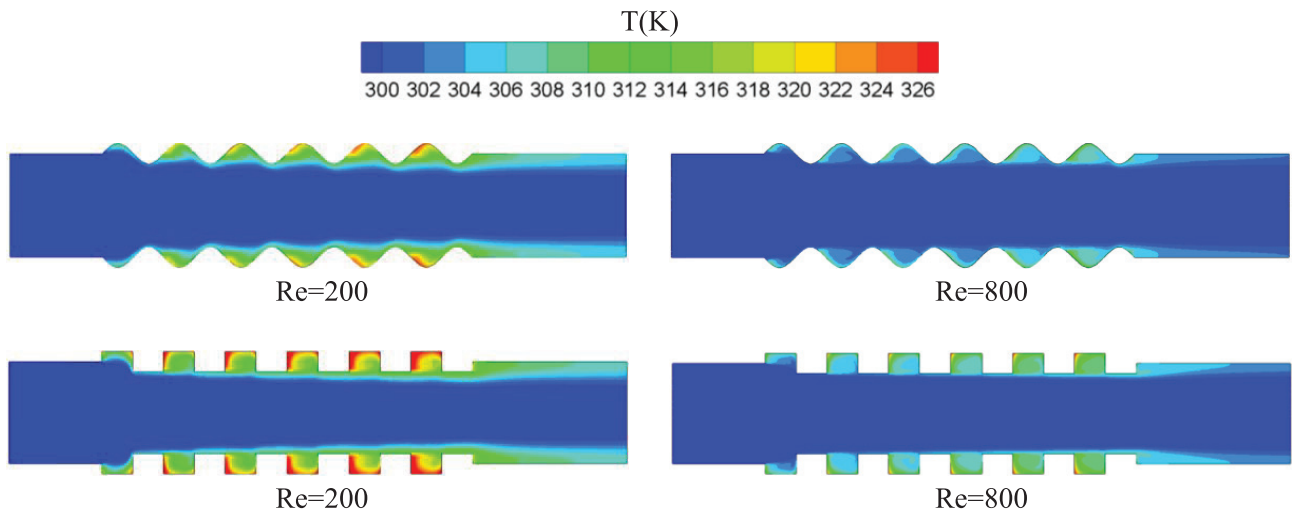


Figure 6. Temperature distribution for Re= 800 and  $\phi= 5\%$ .

resulting from the mixing of the cold fluid in the channel core with the hot fluid near the heated wall. The mixing of the cold and hot fluids near the heated wall is more efficient at higher Reynolds numbers. Moreover, as the Reynolds number increases, the highest cooling effect is produced by the Sinusoidal channel.

**Analysis of Nusselt Number**

The local Nusselt number along the sinusoidal and square channel wall is presented at Figure 7 (a,b) for  $\phi= 5\%$  and Re= 800. We added for each configuration streamline contour. The analysis of this figure shows that heat transfer rate is closely related to the flow pattern behavior. The variations of local Nu number at wavy walls is periodically but with reduced amplitude. We can observe that the local Nusselt numbers of both channels (sinusoidal and square) has a maximum value in the first wave and due to the formation of thermal boundary layer there is a negligible change in the Nusselt number after the tertiary wave of the

channel. Moreover the local Nusselt number increases in the converging section and decreases in the diverging section. A similar trend is obtained in Ref. [22] with  $\phi= 0$ .

**Effects of Nanoparticle Diameter on the Heat Transfer**

The Nusselt number of a nanofluid is impacted by various factors, one of which is the size of the dispersed nanoparticles. Figure 8 illustrates the influence of nanoparticles diameter on the Nusselt number of Al<sub>2</sub>O<sub>3</sub>/water nanofluid at different Reynolds numbers and a constant volume fraction of 5% for both channels. The figure shows that the smallest diameter of nanoparticles (10 nm) results in a higher average Nusselt number compared to 40 and 60 nm. The increase in thermal conductivity resulting from decreasing nanoparticle size enhances convective heat transfer, thereby raising the Nusselt number. This is due to the fact that smaller nanoparticles can penetrate more easily through the thermal and hydrodynamic boundary layers, thereby improving mixing and increasing the heat transfer

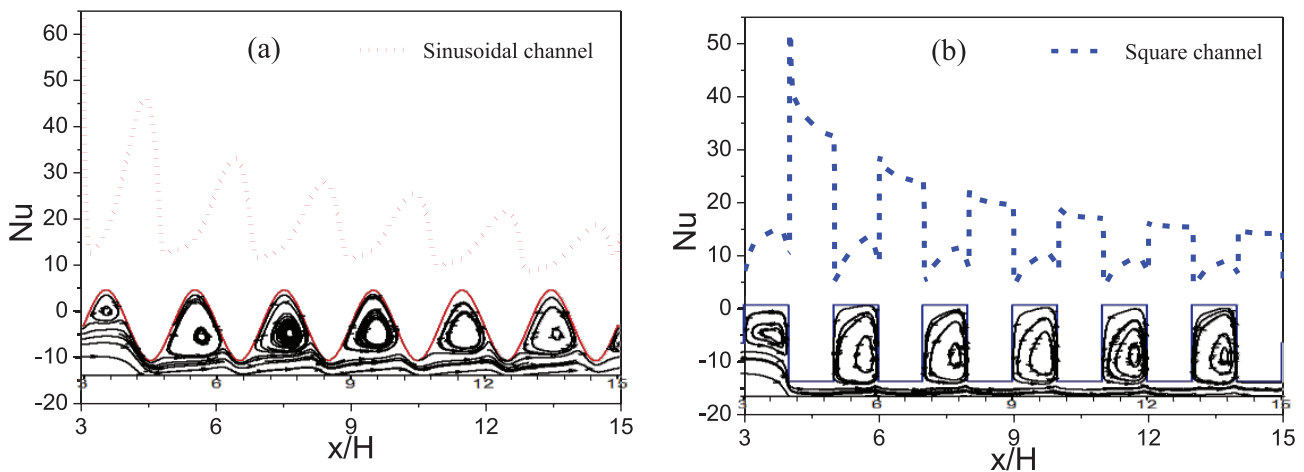
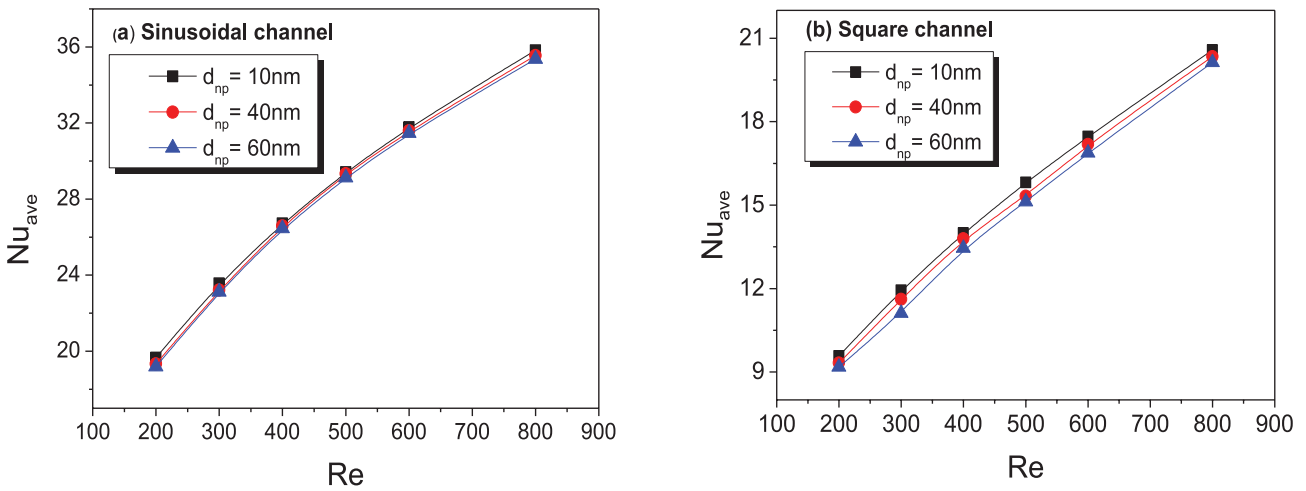


Figure 7. Variation of local Nusselt number along the channels for Re= 800 and  $\phi= 5\%$ .



**Figure 8.** Influence of nanoparticles diameter on the Nusselt number of  $Al_2O_3/water$  nanofluid versus Reynolds number at  $\phi = 5\%$ .

rate. However, the magnitude of this improvement is minor. For instance in case of sinusoidal channel, at a Reynolds number of 800 and a volume fraction of 5%, the increase in the Nusselt number between 10 nm and 40 nm nanoparticle diameters is 0,78%, while the increase between 10 nm and 60 nm is 1,28%, and for  $Re = 200$  the increase between 10 and 40nm is 1,72% but between 10 nm and 60 nm, it is 2.43%.

**Effects of Nanoparticle Concentrations and Reynolds Number on the Heat Transfer**

Based on the results depicted in Figure 9, it is evident that all nanofluids exhibit higher values of  $Nu$  compared to pure water ( $\phi = 0$ ), as an increase in  $\phi$  enhances the fluid’s thermophysical properties (i.e., thermal conductivity and viscosity). The results also demonstrate that an increase in the

$Re$  of nanofluids contributes to a higher  $Nu$  value, primarily due to the significant energy exchange resulting from the chaotic movement of nanoparticles, resulting in improved heat transfer rates as  $Re$  and  $\phi$  increase. Furthermore, increasing  $\phi$  seems to have a more pronounced impact on  $Nu$  when  $Re$  is increased. For instance, in a square channel, when  $\phi$  is 5%, the heat transfer rate improves by 7.03% at  $Re = 800$  compared to  $Re = 200$ , which results in a 3.53% increase in the heat transfer rate. Additionally, the findings illustrate that increasing the volume concentration of  $Al_2O_3/water$  from 1% to 5% at  $d_{np} = 10\text{nm}$  for  $Re = 800$  in the case of the sinusoidal channel led to an improvement of approximately 6.548% in the average Nusselt number. In the case of the square channel, the enhancement was found to be 5.712%. Thus, an increase in the volume fraction of nanoparticles intensifies their interaction and collision,

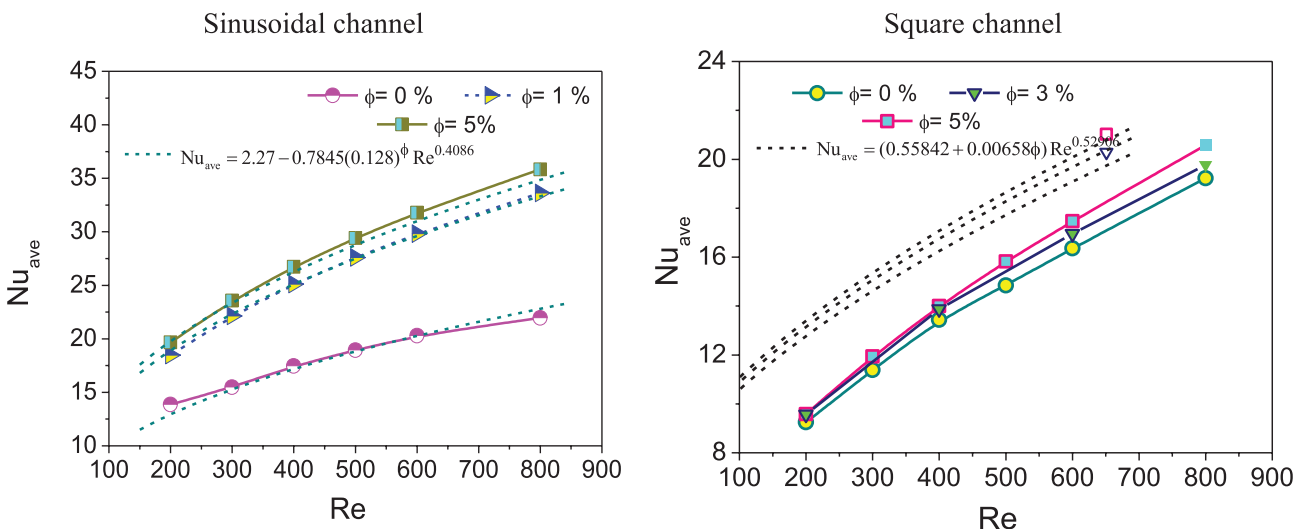


**Figure 9.** Average Nusselt number versus Reynolds number at  $d_{np} = 10\text{nm}$  in Sinusoidal channel and Square channel.

diffusion, and relative movement near the channel walls, resulting in rapid heat transfer from the walls to the nanofluid. In other words, increasing the volume concentration of nanoparticles intensifies the mechanisms responsible for enhanced heat transfer.

Based on obtained data in the current study, two correlations for the average Nusselt number  $Nu$  as a function of Reynolds number and nanoparticles volume fraction has been proposed, respectively for sinusoidal channel and square channel at  $d_{np} = 10\text{nm}$ ,  $0 \leq \phi \leq 0,05$  and  $200 \leq Re \leq 800$ .

$$Nu_{avr} = 2.27 - 0.7845(0.128)^\phi Re^{0.4086} \quad \text{Case of sinusoidal channel}$$

$$Nu_{ave} = (0.55842 + 0.00658\phi) Re^{0.52906} \quad \text{Case of square channel}$$

These correlations were obtained following the curve fitting technique using least-squares method. Very well prediction of the Nusselt number with a maximum error of 6% as shown in Figure 9.

Figure 10 presents the thermo-hydraulic performance (THP). The results indicate that increasing nanoparticle concentration ( $\phi$ ) leads to an increase in THP, and the sinusoidal channel exhibits higher THP than the square channel. The highest THP value is observed for the sinusoidal channel with  $\phi = 5\%$  and  $Re = 800$ .

In this second part of our numerical study, the influence of nanoparticle concentration, channel geometry, Reynolds number, diameter of nanoparticles on the generation of thermal, frictional, total entropy and Bejan number are studied.

### Effects of Channel Geometry and Reynolds Number

The variation of thermal and friction irreversibility versus Reynolds number for both geometry's at  $\phi = 5\%$  with  $d_{np} = 10\text{nm}$

= 10nm of  $Al_2O_3$ /Water nanofluid are displayed in Figure 11. The thermal irreversibility decreases with the increase of Reynolds number in both ducts, the reason is that the Nusselt number increases with an increase in the Reynolds number, which obviously improves the heat transfer performance and hence, leads to a decrease in thermal entropy generation [22], as we notice that the maximum and minimum thermal entropy generation belongs to the square and sinusoidal channel respectively. Likewise, the inverse tendency between thermal and frictional irreversibility for the Reynolds number is apparent in the same figure, where we notice that the frictional irreversibility increases with the Reynolds number, the same result was found by J.A. Esfahani et al. [24]. In addition the variation of friction irreversibility "Sf" between the sinusoidal and square channel is negligible in comparison to the variation of thermal irreversibility "St". As an example: for  $Re = 800$ , Sf (square channel) =  $4.1389E-6 \text{ w/m}^3\text{k}$  and Sf (sinusoidal channel) =  $3.8491E-6 \text{ w/m}^3\text{k}$  which makes a variation of 6.98% on the other hand St (square channel) =  $0.1997 \text{ w/m}^3\text{k}$  and St (sinusoidal channel) =  $0.0948 \text{ w/m}^3\text{k}$  which makes a variation of 52.50%.

### Effects of Nanoparticle Concentration

It is visible from Figure 12a and 12b, as the concentration of  $Al_2O_3$  nanoparticles increases from 0% to 5% for both channels (sinusoidal and square), frictional entropy generation increase because viscosity of nanofluids increases with nanoparticles volume fraction [28]. Additionally, in Figure 12a and 12b, we notice the opposite effect between frictional and thermal irreversibility, the increase of nanoparticle concentration from 0% to 5% diminishes the thermal irreversibility because the effective thermal conductivity of nanofluids increases with the increase in the nanoparticles volume fraction[41], which leads to an improvement in heat

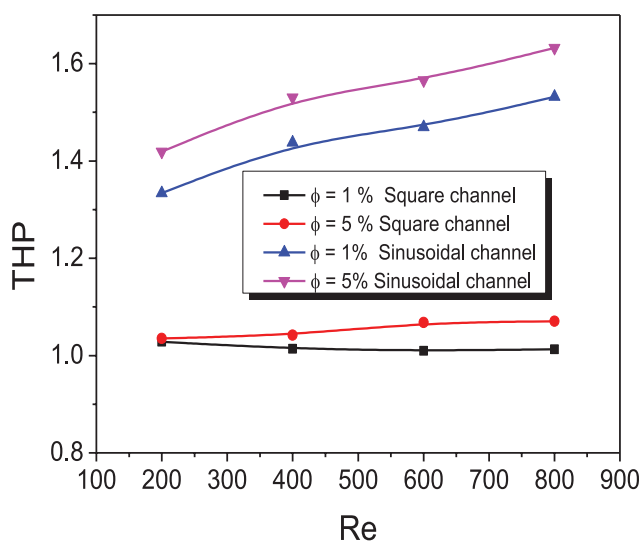


Figure 10. Thermo-hydraulic performance versus Reynolds numbers at  $\phi = 1\%$  and  $\phi = 5\%$ .

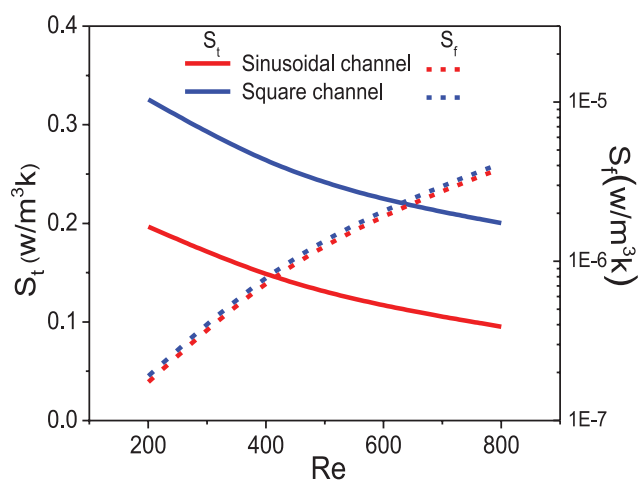
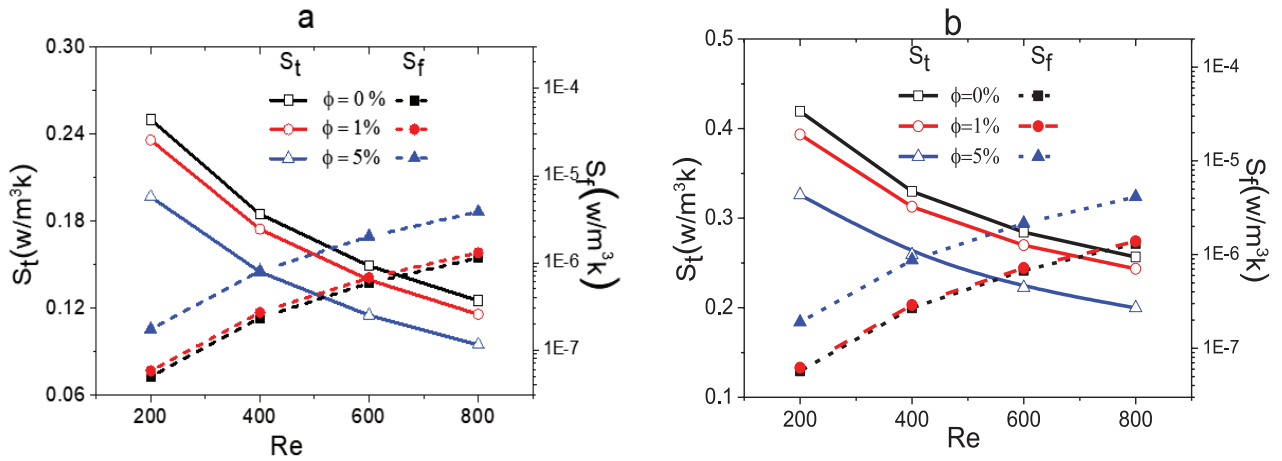


Figure 11. Variation of thermal and frictional irreversibility with respect to Reynolds number for different channels at  $d_{np} = 10\text{nm}$  and  $\phi = 5\%$ .



**Figure 12.** Variation of thermal and frictional irreversibility for different nanoparticles volume fractions at  $d_{np}= 10$  nm in (a) Sinusoidal channel, (b) Square channel.

transfer between the wall and the fluid and a decrease in thermal entropy, thereby, the behavior of total entropy generation is dominated by thermal effects and the frictional entropy is negligible. Similar results that show a reduction in total entropy with the addition of nanoparticles in water- $Al_2O_3$  nanofluid have been reported by [42, 43].

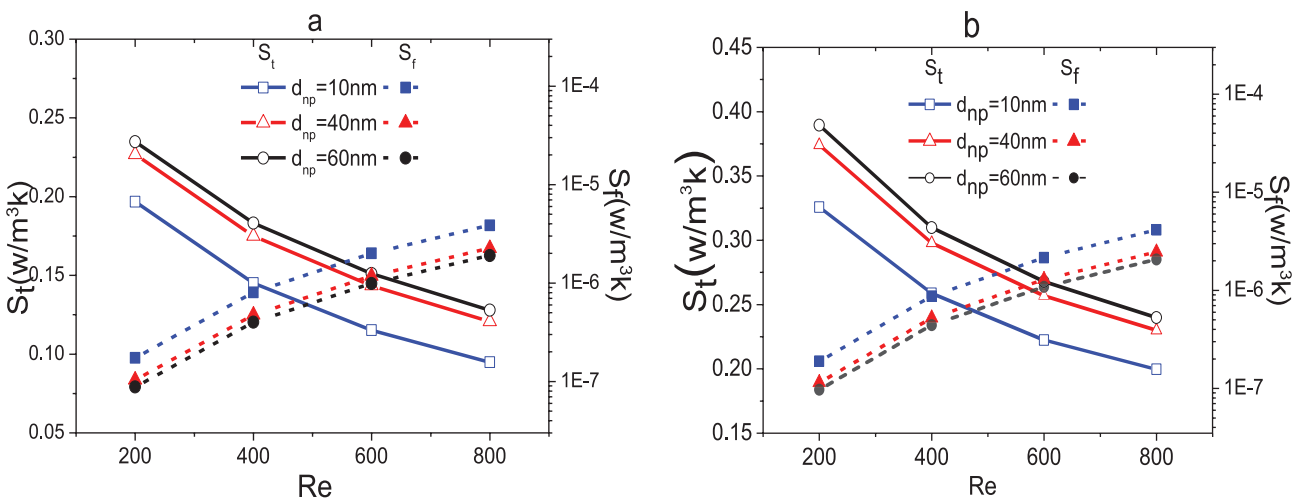
**Effect of Nanoparticle Diameter**

Figure 13 show the effect of nanoparticle diameter on thermal and frictional entropy generation, which is rarely studied. According to our results, we conclude that the increase in particle size leads to an increase in thermal entropy generation and a decrease in frictional entropy generation, which is due to the decrease in the effective viscosity (see equation 16 which shows that the frictional entropy generation is proportional to the viscosity associated with

the diameter of the nanoparticles. (Equation (11) shows that the effective viscosity which is estimated in this article using the Rudyak model, decreases as the nanofluid particle size increases). Similar results on effect of nanoparticle diameter on thermal and frictional entropy generation were found by [23].

Figure 14 illustrates that the sinusoidal channel exhibits a lower total entropy generation compared to the square channel due to the presence of enhanced heat transfer and decreased thermal boundary layer in the former.

As observed in Figure 15, reducing the diameter of nanoparticles in the nanofluid results in a reduction in the total entropy generation. This is due to the fact that smaller nanoparticles have a larger surface-to-volume ratio, which increases the interfacial area between the nanoparticles and the base fluid, leading to enhanced heat transfer. As



**Figure 13.** Frictional and thermal entropy generation for various nanoparticles diameter at  $\phi= 5\%$  in (a) Sinusoidal channel, (b) Square channel.

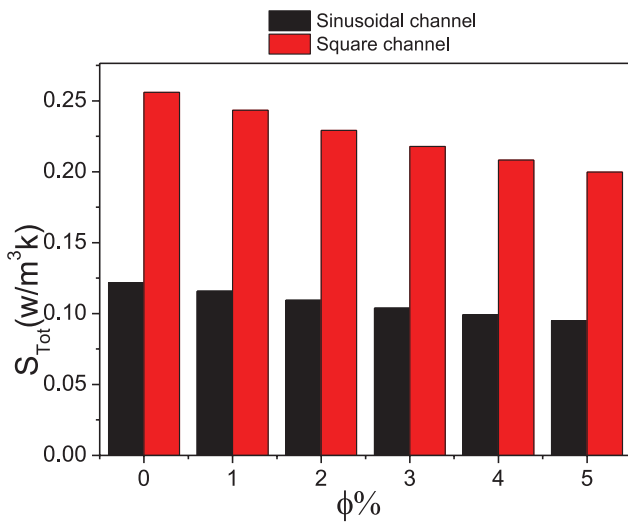


Figure 14. Variations of the total entropy generation with nanoparticle concentration for different channels at  $d_{np}=10\text{nm}$  and  $Re=800$ .

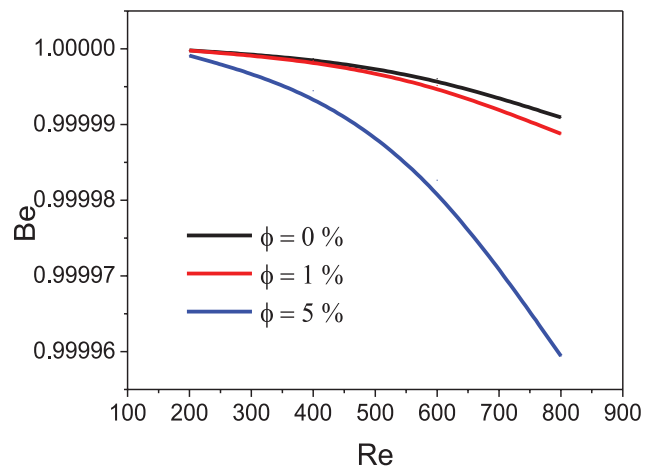


Figure 16. Effect of nanoparticle concentration on Bejan number at different Reynolds for  $d_{np}=10\text{nm}$  in sinusoidal channel.

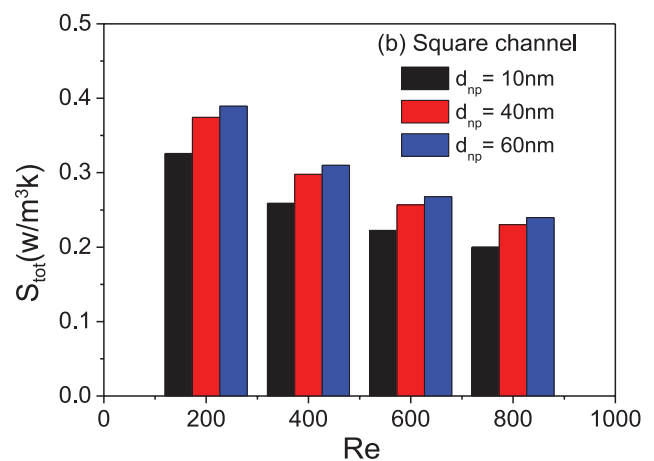
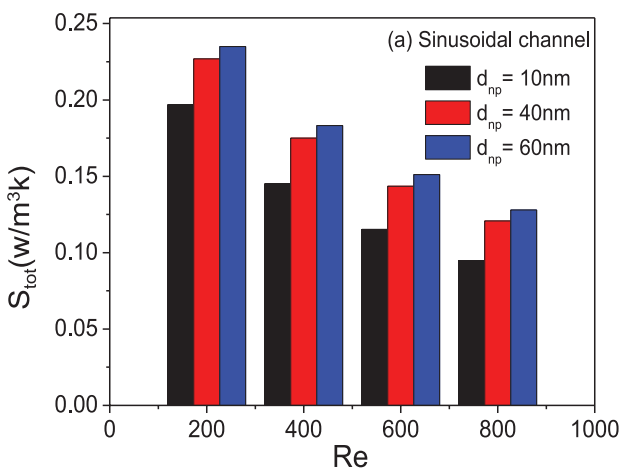


Figure 15. Variations of the total entropy generation versus Reynolds number with nanoparticle diameter at  $\phi=5\%$  for sinusoidal and square channel.

a result, the temperature gradient between the nanoparticles and the fluid is reduced, which subsequently leads to lower entropy generation. Moreover, the decrease in total entropy with the reduction in nanoparticle diameter is more prominent in the sinusoidal channel. For instance, when  $\phi=5\%$ ,  $Re=800$ , and the  $d_{np}$  decreases from 60nm to 10nm, the total entropy generation experiences a reduction of 34,85% in the sinusoidal channel and 20,05% in the square channel.

The data presented in Figure 16 demonstrates the impact of varying values of  $\phi$  on the Bejan number ( $Be$ ) across different  $Re$  values for the sinusoidal channel. The results reveal that as  $\phi$  and  $Re$  values increase,  $Be$  values decrease. This decline can be attributed to an increase in

frictional entropy generation and a decrease in thermal entropy generation, as indicated by Figure 12a. In contrast, in the square channel,  $Be$  is almost equal to 1 due to the predominance of thermal entropy generation, with frictional entropy generation being relatively insignificant in comparison.

### CONCLUSION

The application field of “Entropy generation of  $Al_2O_3$  / water nanofluid in corrugated channels” is in the area of heat transfer and fluid mechanics. Specifically, the study focuses on analyzing the entropy generation of  $Al_2O_3$ /water nanofluid in corrugated channels, which are commonly

used in heat exchangers and cooling systems. The findings of this study can be applied in the optimization and design of heat transfer systems, leading to improved efficiency and reduced energy consumption. The results obtained can also be useful in the development of more efficient cooling systems for various industrial applications.

The results of this study led to the following detailed conclusions:

- The regions of recirculation exhibit greater flow disturbances, which contribute significantly to both enhancing heat transfer and generating viscous irreversibility.
- The study proposed correlations for the average Nusselt number for both sinusoidal and square channels.
- This study found that increasing the concentration of nanoparticles in the nanofluid can reduce thermal entropy generation but increase frictional entropy generation. This effect is more pronounced for concentrations greater than 1%.
- A recommendation is made to use smaller nanoparticles since a decrease in particle size can improve heat transfer while minimizing thermal entropy and increasing frictional entropy.
- By reducing the diameter of nanoparticles in the nanofluid, the total entropy generation is reduced.
- As the Reynolds number increases for both sinusoidal and square channels, there is a corresponding increase in frictional entropy generation and a decrease in thermal entropy generation.
- The thermal entropy generation plays a more significant role in the total entropy generation compared to frictional entropy generation, which is considered to be negligible.
- The study found that the square channel generates the highest entropy, while the sinusoidal channel generates the lowest entropy, making the sinusoidal channel a more suitable geometry.
- The results of this study show that Bejan number ( $Be$ ) is almost equal to 1 in the square channel due to the predominance of thermal entropy generation.

Thus, the possible main contributions of this study could be:

- In order to minimize the rate of entropy generation, it is recommended that researchers use  $Al_2O_3$  /Water nanofluid in a sinusoidal channel with a small diameter and high concentrations of nanoparticles, instead of using the square channel.
- Provide insight into the thermodynamic behavior of the  $Al_2O_3$ /water nanofluid in complex geometries, which could be useful for optimizing heat transfer in various applications.
- Identify the effects of key parameters such as Reynolds number, nanoparticle concentration, and channel geometry on entropy generation in flows of the  $Al_2O_3$ /water nanofluid.

The future directions following the contributions of this paper are:

- 1- Study of forced convection and entropy generation of hybrid nanofluids through corrugated channels in porous media.
- 2- Using other base fluids (ethylene glycol, oil) in the study of heat transfer and entropy generation in complex geometries.
- 3- Study of entropy generation of a non-Newtonian nanofluid, taking into consideration the effect of the diameter and shape of the nanoparticles.
- 4- Studying the impact of different boundary conditions, such as varying wall temperatures or heat fluxes, on entropy generation in nanofluid flows, to account for more realistic scenarios in practical applications.
- 5- Developing new theoretical models or experimental techniques to quantify the contribution of various sources of irreversibility in nanofluid flows, and exploring ways to reduce or mitigate them.

## AUTHORSHIP CONTRIBUTIONS

Authors equally contributed to this work.

## DATA AVAILABILITY STATEMENT

The authors confirm that the data that supports the findings of this study are available within the article. Raw data that support the finding of this study are available from the corresponding author, upon reasonable request.

## CONFLICT OF INTEREST

The author declared no potential conflicts of interest with respect to the research, authorship, and/or publication of this article.

## ETHICS

There are no ethical issues with the publication of this manuscript.

## NOMENCLATURE

$C_p$	Specific heat (J/kg K)
$D$	Diameter of the tube [m]
$d_{np}$	Diameter of the nanoparticles [nm]
$dbf$	Diameter of a water molecule
$k$	Thermal conductivity [W/m.K]
$K_b$	Boltzmann constant
$Nu$	Nusselt number
$r$	Radius
$q_w$	Heat flux at the wall [W/m <sup>2</sup> ]
$Re$	Reynolds number
$S_f$	Frictional entropy generation [W/m <sup>3</sup> .K]
$S_t$	Thermal entropy generation [W/m <sup>3</sup> .K]
$Stot$	Total entropy generation [W/m <sup>3</sup> .K]
$T$	Temperature [K]

Tb	Fluid average bulk temperature[K]
Tfr	Freezing point of the base liquid[K]
Tw	Wall temperature[K]
u,v	Velocity components[m]
x,r	Axial and radial coordinates [m]

Greek symbols

$\rho$	Density (kg/m <sup>3</sup> )
$\mu$	Viscosity (kg/m s)
$\phi$	Nanoparticle volume fraction(%)

Subscripts

bf	Refers to base fluid
in	Refers to inlet
nf	Refers to nanofluid
np	Refers to nanoparticles
p	Refers to particles

REFERENCES

- [1] Hamza NFA, Aljabair S. Review of Heat transfer enhancement using hybrid nano fluid or twisted tape insert. *J Mech Eng Res Dev* 2021;44:345–357.
- [2] Ahmed SH, Abdulhassan AK, Sattar A. Review of computational multi-phase approaches of nano-fluids filled systems. *Therm Sci Eng Progress* 2022;28:101–175. [\[CrossRef\]](#)
- [3] Taşkesen E, Tekir M, Pazarlıoğlu HK, Gurdal M, Gedik E, Arslan, K. The effect of MHD flow on hydrothermal characteristics of ferro-nano-fluid in circular pipe. *Experimental Heat Transfer* 2022;36:617–631. [\[CrossRef\]](#)
- [4] Insiat IR, Hossain F, Shafwat AS, Sadrul Islam AKM. Numerical simulation on performance evaluation among metal and oxide based nanofluids for power savings application of a circular tube. *J Therm Eng* 2021;7:1150–1162. [\[CrossRef\]](#)
- [5] Hamza NFA, Aljabair S. Evaluation of thermal performance factor by hybrid nanofluid and twisted tape inserts in heat exchanger. *Heliyon* 2022;8:e11950. [\[CrossRef\]](#)
- [6] Ekiciler R. A CFD investigation of Al<sub>2</sub>O<sub>3</sub>/water flow in a duct having backward-facing step. *J Therm Eng* 2019;5:31–41. [\[CrossRef\]](#)
- [7] Aljabair S, Mohammed AA, Alesbe I. Natural convection heat transfer in corrugated annuli with H<sub>2</sub>O-Al<sub>2</sub>O<sub>3</sub> nanofluid. *Heliyon* 2020;6:e05568. [\[CrossRef\]](#)
- [8] Kaya H, Alkasem M, Arslan K. Effect of nanoparticle shape of Al<sub>2</sub>O<sub>3</sub>/Pure Water nanofluid on evacuated U-Tube solar collector efficiency. *Renew Energy* 2020;162:267–284. [\[CrossRef\]](#)
- [9] Ekiciler R, Çetinkaya MSA, Arslan K. Heat transfer enhancement in an equilateral triangular duct by using an Al<sub>2</sub>O<sub>3</sub>/water nanofluid: Effect of nanoparticle shape and volume fraction. *Heat Transf Res* 2020;51:741–757. [\[CrossRef\]](#)
- [10] Kurtulmuş N, Sahin B. A review of hydrodynamics and heat transfer through corrugated channels. *Int Commun Heat Mass Transf* 2019;108:10430. [\[CrossRef\]](#)
- [11] Wang CC, Chen CK. Forced convection in a wavy-wall channel. *Int J Heat Mass Transf* 2002;45:2587–2595. [\[CrossRef\]](#)
- [12] Aljabair S, Ekaid AL, Ibrahim SH, Alesbe I. Mixed convection in sinusoidal lid driven cavity with non-uniform temperature distribution on the wall utilizing nanofluid. *Heliyon* 2021;7:e06907. [\[CrossRef\]](#)
- [13] Gürsoy E, Pazarlıoğlu HK, Dağdeviren A, Gürdal M, Gedik E, Arslan K, Kurt H. Energy analysis of magnetite nanofluid flowing in newly designed sudden expansion tube retrofitted with dimpled fin. *Int J Heat Mass Transf* 2022;199:123446. [\[CrossRef\]](#)
- [14] Habeeb AS, Aljabair S, Karamallah AA. Experimental and numerical assessment on hydrothermal behaviour of MgO-Fe<sub>3</sub>O<sub>4</sub>/H<sub>2</sub>O hybrid nano-fluid. *Int J Thermofluids* 2022;16:100231. [\[CrossRef\]](#)
- [15] Hamza NFA, Aljabair S. Numerical and experimental investigation of heat transfer enhancement by hybrid nanofluid and twisted tape. *Eng Technol J* 2023;41:69–85. [\[CrossRef\]](#)
- [16] Albojamal A, Hamzah H, Haghghi A, Vafai K. Analysis of nanofluid transport through a wavy channel. *Numerical Heat Transfer, Part A: Applications* 2017;72:869–880. [\[CrossRef\]](#)
- [17] Heidary H, Kermani MJ. Effect of nano-particles on forced convection in sinusoidal-wall channel. *Int Commun Heat Mass Transf* 2010;37:1520–1527. [\[CrossRef\]](#)
- [18] Mahian O, Kianifar A, Kleinstreuer C, Al-Nimr MA, Pop I, Wongwises S, Sahin AZ. A review of entropy generation in nanofluid flow. *Int J Heat Mass Transf* 2013;65:514–532. [\[CrossRef\]](#)
- [19] Taskesen E, Tekir M, Gedik E, Arslan K. Numerical investigation of laminar forced convection and entropy generation of Fe<sub>3</sub>O<sub>4</sub>/water nanofluids in different cross sectioned channel geometries. *J Therm Eng* 2021;7:1752–1767. [\[CrossRef\]](#)
- [20] Pazarlıoğlu HK, Gürsoy E, Gürdal M, Tekir M, Gedik E, Arslan K, Taşkesen E. The first and second law analyses of thermodynamics for coFe<sub>2</sub>O<sub>4</sub>/H<sub>2</sub>O flow in a sudden expansion tube inserted elliptical dimpled fins. *Int J Mech Sci* 2023;246:108144. [\[CrossRef\]](#)
- [21] Pazarlıoğlu HK, Ekiciler R, Arslan K, Mohammed NAM. Exergetic, energetic, and entropy production evaluations of parabolic trough collector retrofitted with elliptical dimpled receiver tube filled with hybrid nanofluid. *Appl Therm Eng* 2023;223:120004. [\[CrossRef\]](#)
- [22] Akbarzadeh M, Rashidi S, Esfahani JA. Influences of corrugation profiles on entropy generation heat transfer, pressure drop, and performance in a wavy channel. *Appl Therm Eng* 2017;116:278–291. [\[CrossRef\]](#)

- [23] Rashidi S, Akbarzadeh M, Masoodi R, Languri EM. Thermal-hydraulic and entropy generation analysis for turbulent flow inside a corrugated channel. *Int J Heat Mass Transf* 2017;109: 812–823. [\[CrossRef\]](#)
- [24] Esfahani, JA, Akbarzadeh, M, Rashidi, S, Rosen, MA, Ellahi R. Influences of wavy wall and nanoparticles on entropy generation over heat exchanger plat. *Int J Heat Mass Transf* 2017;109:1162–1171. [\[CrossRef\]](#)
- [25] Hudhaifa H, Besir Sahin S. Analysis of SWCNT-water nanofluid flow in wavy channel under turbulent pulsating conditions: Investigation of homogeneous and discrete phase models. *Int J Therm Sci* 2023;184:108011. [\[CrossRef\]](#)
- [26] Boudraa B, Bessaih R. Heat transfer and entropy generation of water/TiO<sub>2</sub> nanofluid flow in a wavy channel using two-phase mixture approach. *Thermophys Aeromechanics* 2022;29:587–604. [\[CrossRef\]](#)
- [27] Ehsan E-B, Moghadam MC, Niazmand H, Daungthongsuk W, Wongwises S. Experimental and numerical investigation of nanofluids heat transfer characteristics for application in solar heat exchangers. *Int J Heat Mass Transf* 2016;92:1041–1052. [\[CrossRef\]](#)
- [28] Omri M, Bouterra M, Ouri H, Kolsi L. Entropy generation of nanofluid flow in hexagonal microchannel. *J Taibah Univ Sci* 2022;16:75-88. [\[CrossRef\]](#)
- [29] Saha G, Paul MC. Numerical analysis of the heat transfer behavior of water-based Al<sub>2</sub>O<sub>3</sub> and TiO<sub>2</sub> nanofluids in a circular pipe under the turbulent flow condition. *Int Commun Heat Mass Transfer* 2016;56:96–108. [\[CrossRef\]](#)
- [30] Pak BC, Cho YI. Hydrodynamic and heat transfer study of dispersed fluids with submicron metallic oxide particles. *Exp Heat Transf Int J* 1998;11:151–170. [\[CrossRef\]](#)
- [31] Xuan Y, Roetzel W. Conceptions for heat transfer correlation of nanofluids. *Int J Heat Mass Transfer* 2000;43:3701–3707. [\[CrossRef\]](#)
- [32] Corcione, M. Empirical correlating equations for predicting the effective thermal conductivity and dynamic viscosity of nanofluids. *Energy Convers Manag* 2011;52:789–793. [\[CrossRef\]](#)
- [33] Rudyak VY. Viscosity of nanofluids - why it is not described by the classical theories. *Adv Nano* 2013;2:266–279. [\[CrossRef\]](#)
- [34] Bejan A. General criterion for rating heat-exchanger performance. *Int J Heat Mass Transf* 1978;21:655–658. [\[CrossRef\]](#)
- [35] Bejan A. Study of entropy generation in fundamental convective heat transfer. *J Heat Trans* 1979;101:718–725. [\[CrossRef\]](#)
- [36] Haseli Y. *Entropy Analysis in Thermal Engineering Systems Book*. Cambridge, Massachusetts: Imprint Academic Press; 2018. p. 202.
- [37] Basak T, Kaluri RS, Balakrishnan A. Effects of thermal boundary condition on entropy generation during natural convection. *Numer Heat Transf Part A* 2011;59:372–402. [\[CrossRef\]](#)
- [38] Patankar SV. *Computation of Conduction and Duct Flow Heat Transfer*. New York: Hemisphere Publishing Corporation; 1988.
- [39] ANSYS Inc. *Fluent User Guide and Fluent Theory Guide*, version 16.0. ANSYS Inc.
- [40] Ahmed MA, Yusoff MZ, Ng KC, Shuaib NH. Numerical and experimental investigations on the heat transfer enhancement in corrugated channels using SiO<sub>2</sub>-water nanofluid. *Case Studies in Thermal Engineering* 2015;6:77–92. [\[CrossRef\]](#)
- [41] Sarviya RM, V Fuskele. Review on thermal conductivity of nanofluids. *Mater Today Proc* 2017;4:4022–4031. [\[CrossRef\]](#)
- [42] Moghaddami M, Shahidi S, Siavashi M. Entropy generation analysis of nanofluid flow in turbulent and laminar regimes. *J Comput Theor Nanosci* 2012;9:1586–1595. [\[CrossRef\]](#)
- [43] Bianco V, Manca O, Nardini S. Entropy generation analysis of turbulent convection flow of Al<sub>2</sub>O<sub>3</sub>-water nanofluid in a circular tube subjected to constant wall heat flux. *Energy Convers Manag* 2014;77:306–314. [\[CrossRef\]](#)